Antiferromagnetism and Low Magnetostriction in $Fe100_{-x}Mn_x$ (x = 38, 42, 46, 50, and 55) Alloys

Reiko Sato-Turtelli, Cristina Bormio-Nunes, K. T. Tiguman, David Geist, A. Panigrahi, Cristina Grijalva, Stephan Sorta, Roland Grössinger and Michael Zehetbauer.

Abstract

The structural and magnetic properties of polycrystalline Fe_{100-x}Mnx alloys with x = 38, 42, 46, 50, and 55 atomic percent were investigated after a heat treatment and a cold rolling process. According to X-ray diffraction (XRD), all samples crystallize into a γ -phase. For cold rolled alloys x = 38 and 42, XRD analysis using pole figures showed no texture formation whereas cold rolled alloys with x = 46 and 50 exhibited texture components {110} <1–12> and with x = 55, {011} <01–1>. Magnetization measurements clearly demonstrate an antiferromagnetic type of ordering. For both the as-cast as well as the cold rolled materials, magnetostriction measurements at room temperature gave nearly zero magnetostriction.

Index Terms: Antiferromagnetism, Fe-Mn, Magnetostriction.

Introduction

Fe–Mn alloys exhibit in the equiatomic region antiferromagnetic ordering with Néel temperatures ~450 K (187 °C). According to the phase diagram, these alloys with Mn concentrations ranging from 14 to 55 at % (at 600 °C) and 4% to 61% (at 800 °C) crystallize into a single fcc γ -phase. Ishikawa and Endoh [1] reported that a maximum value of T_N is found between 20% and 60% of Mn, and a minimum magnetic moment occurs for concentrations ~50% Mn. Peng and Zhang [2] found in polycrystalline

$Fe_{58}Mn_{42}$ a high magnetostriction of 169 ppm at room temperature applying a magnetic field of 1 T, and under a compressive stress of 1.52 MPa an improved magnetostriction of 581 ppm [2]. Later, Zhang et al. [3] found a larger magnetostriction of 690 ppm at 1350 kA/m in the same alloy in the as-cast state, however, a decreased magnetostriction was obtained after annealing the sample at 1100 °C for 24 h. This decrease of the magnetostriction was attributed to the separation of the austenite single γ -phase into a mixture containing fcc γ -phase, hcp ε-phase, and a body bcc α-phase after isothermal heat treatment [3]. The same authors investigated the magnetostriction of polycrystalline $Fe_{50}Mn_{50}$ and found in the as-cast sample a magnetostriction of 500 ppm and a giant magnetostriction of 2100 ppm when the sample was cold rolled and annealed at 600 °C for 1 h [4]. They concluded that the preferred <110> orientation formed along the rolling direction (RD) during the deformation is responsible for the improvement in magnetostriction. The importance of the formation of single γ -phase and a preferential crystal orientation in $Fe_{50}Mn_{50}$ is also reported in [5]. In this paper, they obtained a magnetostriction of 300 ppm for the as-cast sample and a large magnetostriction of 750 ppm in wire obtained by combining hot rolling and cold drawing processes.

To perform a more systematic study on $Fe_{100-x}Mn_x$ alloys, in this paper, the magnetostriction of $Fe_{100-x}Mn_x$ with different content of Mn (x = 38, 42, 46, 50, and 55) in annealed and cold-rolled states was investigated. For this purpose, for the as-cast samples, careful composition determinations and structural characterizations were performed. Measurements of the temperature dependence of the initial susceptibility and the magnetization were performed to define the type of order.

Experiment

For the melting process, Fe was laminated and cut into strips and Mn was crushed to obtain Mn powder. For Mn, a mass excess of 5% in weight was added to compensate the evaporation losses during melting in the arc furnace. Ingots of Fe–Mn alloys with 8 g each were arc melted three times to ensure chemical homogeneity. The compositions of the $Fe_{100-x}Mn_x$ alloys were chosen as x = 38, 42, 46, 50, and 55, where x is the atomic percentage of manganese. Part of each ingot was annealed at 1000 °C for 72 h. To retain the γ -phase, the samples were quenched from 1000 °C into water at RT. Concentration analysis of metallic elements were performed to determine the precise compositions of the alloys using an atomic absorption spectrometer PerkinElmer, model Analyst 800, with an integrated system of graphite furnace and flame. Pieces of samples having ~0.1 g were cleaned chemically and physically using the reagents of analytical purity and ultrasound, respectively. The microstructures of the samples were investigated using a TM3000 Hitachi Tabletop Microscope scanning electron microscope and a Panalytical diffractometer, model Empyrean, with copper radiation, nickel filter, voltage 40 kV and current of 30 mA.

TABLE I
ANALYTICAL RESULTS OF CHEMICAL COMPOSITIONS BY ATOMIC ABSORPTION SPECTROPHOTOMETRY

Sample Nominal Composition	Concentration (at %)		Uncertainty (at %)	
	Fe	Mn	Fe	Mn
$Fe_{62}Mn_{38}$	62.84	37.05	0.25	0.20
$Fe_{58}Mn_{42}$	58.70	41.17	0.25	0.22
$Fe_{54}Mn_{46}$	54.24	45.33	0.29	0.22
$Fe_{50}Mn_{50}$	50.11	49.30	0.30	0.24
$Fe_{45}Mn_{55}$	44.24	55.45	0.31	0.25

For the texture analysis, the specimen was mechanically polished by 25% in thickness by P 4000 grade paper. X-ray diffraction (XRD) measurements were conducted in an AXS BRUKER D8 diffractometer with GADDS area detector NANOSTAR, at room temperature with Co-K_a radiation with spot size of 0.8 mm and integrated over an area of 2 mm × 2 mm in continuous scan mode. The distribution of diffraction intensities from three crystal planes {1 1 1}, {2 0 0}, and {2 2 0}were measured on sheet surface parallel to rolling plane. The texture data were processed through software LABOTEX.

The magnetization measurements were performed using a physical property measurement system integrated with vibrating sample magnetometer), from quantum design. The magnetic susceptibility was measured as a function of temperature applying a field of 8×10^4 A/m, and the field dependence of the magnetization at 100, 200, 300, and 400 K was measured up to 7.5×10^6 A/m (9 T). Longitudinal and transverse magnetostriction measurements of all samples were performed at room temperature by a strain gauge method using an ac bridge (50 kHz bridge; HBM type KWS 85A1), in a pulsedfield magnetometer, which exhibits a maximum magnetic field of 4.2×10^6 A/m at a pulse duration of 50 ms. The magnetostriction was also measured using a microcapacitance dilatometer [6]. After all measurements mentioned above, the samples were subjected to 70% cold rolling at room temperature and, applying a magnetic field parallel to the deformation direction, the transversal and perpendicular magnetostrictions were measured by strain gauges.

Results and discussion

Table I shows the results of composition analysis in the arc melted $Fe_{100-x}Mn_x$ alloys with x = 38, 42, 46, 50, and 55. As can be observed in Table I, the Mn concentrations of alloys (except for x = 55) are a bit lower than the nominal values although a mass excess of 5% of Mn was added to produce the samples. The loss is higher for Fe richer alloys because although the melting temperature of Fe is higher than that of Mn the evaporation heat of Mn is higher than that of Fe.

Fig. 1 shows SEM micrographs of the undeformed samples. Only one phase can be identified in all samples. The sample with 55% of Mn shows a structure with more refined and elongated grains. The visible grain size is 100 μm and even larger.

XRD patterns of the samples (before the rolling process) are shown in Fig. 2. For comparison, in this figure, the standard patterns of the body-centered-cubic α-phase, face-centered-cubic γ -phase, and hexagonal closed-packed ε-phase are also presented [7]. Our results indicate that the main phase present in our samples is the γ -phase.

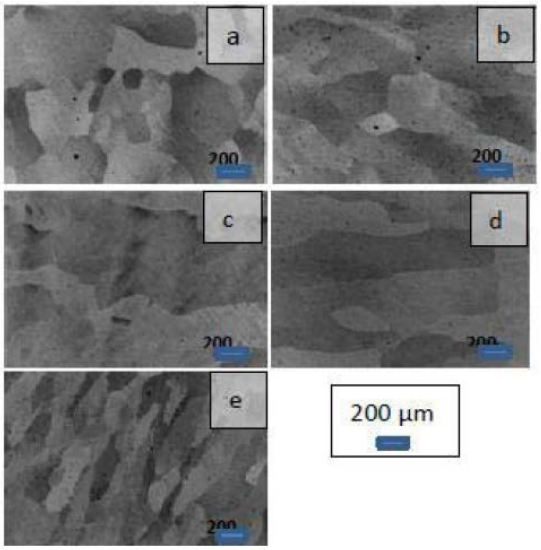

Fig. 1. SEM micrographs of $Fe_{100-x}Mn_x$ alloys with (a) x = 38, (b) 42, (c) 46, (d) 50, and (e) 55.

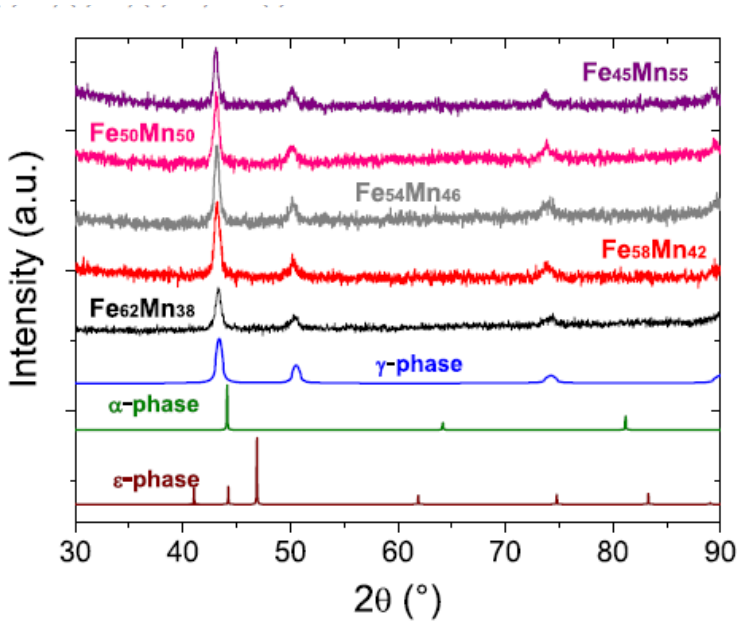

Fig. 2. XRD patterns of $Fe_{100-x}Mn_x$ alloys with x = 38, 42, 46, 50, and 55. The standard diffraction patterns of the α-, γ-, and ε-phases are also shown [6].

Fig. 3 shows the pole figures for the sample with x = 50 and Fig. 4 for the sample with x = 55, after the rolling process. The center of the pole figures corresponds to the direction normal to the specimen surface (ND). The top and the right of the pole figures correspond to the RD and the transverse direction, respectively.

In samples with Mn content lower or equal to x = 42, no significant textures have been observed. For larger contents of Mn including $Fe_{50}Mn_{50}$ (Fig. 3), the texture component is {110} <1–12> typical of a cold rolled material; however, the rolling orthorhombic symmetry is not observed for these cases. Surprisingly, in $Fe_{45}Mn_{55}$, the texture component is different, i.e., equal to {011} <01–1> (Fig. 4), meaning that the RD in this material is parallel to the < 01–1> direction.

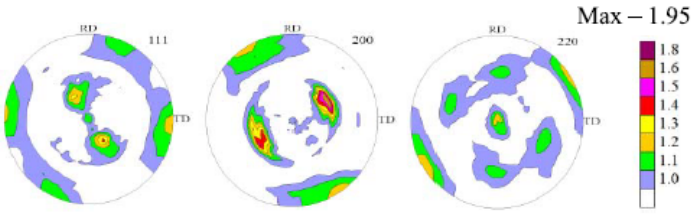

Fig. 3. {111}, {200}, and {220}pole figures of cold rolled $Fe_{50}Mn_{50}$.

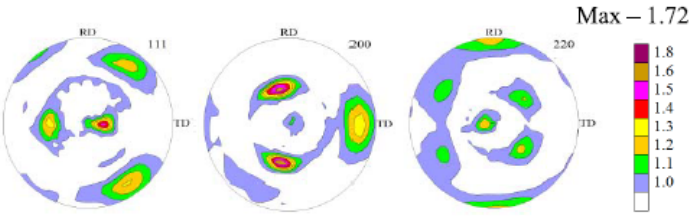

Fig. 4. {111}, {200}, and {220}pole figures of cold rolled $Fe_{45}Mn_{55}$.

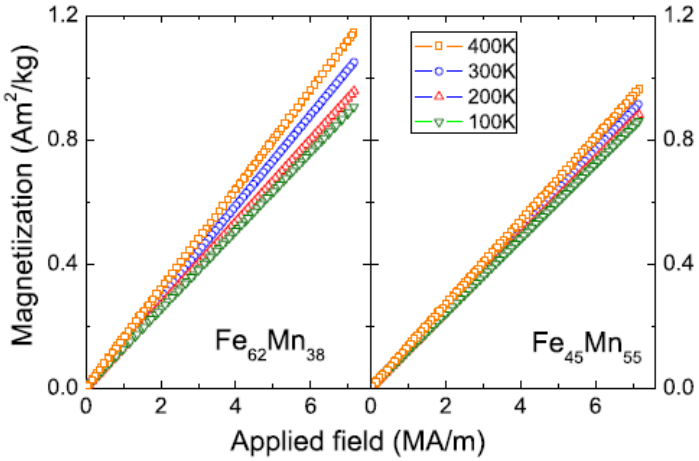

Fig. 5. Magnetization as a function of applied field of $Fe_{62}Mn_{38}$ and $Fe_{45}Mn_{55}$.

It can be summarized that the texture evolution during rolling depends on the Mn content: while with contents up to 42% Mn no distinct texture could be observed, from 46% to 50% Mn a texture component {110 }< 1–12> is clearly observed, but with 55% Mn, another texture component (with about the same intensity) {011 }< 01–1> is found.

The magnetization of all alloys increases linearly with applied field up to 7.5 MA/m, and the slope increases also with temperature indicating that these compounds

are antiferromagnetically ordered. As examples, in this paper, the magnetization as a function of the applied field measured on $Fe_{62}Mn_{38}$ and $Fe_{45}Mn_{55}$ at 100, 200, 300, and 400 K are shown in Fig. 5. The other samples exhibit a similar behavior; however, as expected, the magnetization decreases with increasing Mn content.

The magnetic susceptibility, χ, as a function of the temperature is shown in Fig. 6. Small peaks appearing <60 K are due to the experimental problems on moisture control. The susceptibility increases with increasing temperature like in magnetization measurements, however, in the sample $Fe_{62}Mn_{38}$ a magnetic ordering at 100 K is observed. This ordering temperature corresponds to the Neel temperature, T_N , of metallic α-Mn, which above T_N becomes paramagnetic with a mass magnetic susceptibility of 1.21×10^{-7} m^3/kg [8].

Fig. 7(a) and (b) shows the longitudinal and transverse magnetostrictions as a function of the applied field measured at room temperature by strain gauge (up to 4 MA/m ~5 T) and mini-capacitance dilatometer (up to 0.96 MA/m ~1.2 T), respectively. The magnetostriction was measured on annealed $Fe_{100-x}Mn_x$ (x = 38, 42, 46, 50, and 55) samples. The measurements using the strain gauge are very noisy, but the average longitudinal and transverse magnetostriction values are essentially zero; for both techniques. Our results are not in agreement with the results reported in [2]–[4], although our samples are practically single γ -phase, which condition was imposed in [2]–[4] for obtaining a huge magnetostriction.

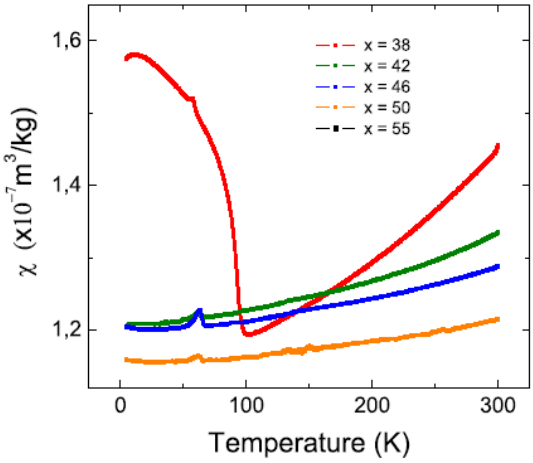

Fig. 6. DC susceptibility versus temperature of $Fe_{100-x}Mn_x$ alloys (x = 38, 42, 46, 50, and 55).

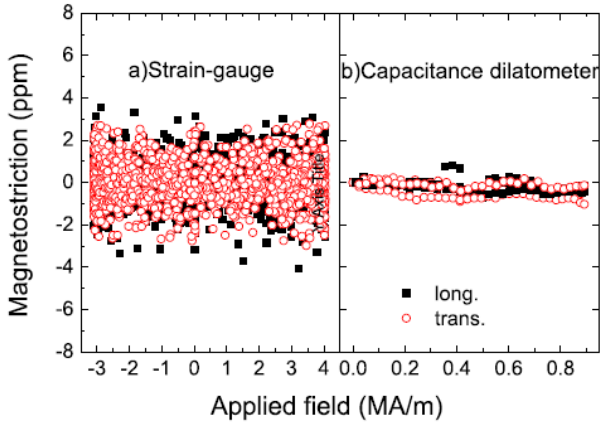

Fig. 7. Magnetostriction of all $Fe_{100-x}Mn_x$ (x = 38, 42, 46, 50, and 55) annealed samples measured with (a) strain gauge and (b) mini-capacitance dilatometer.

Generally, a high magnetostriction is related to a high magnetization and a strong orbital contribution, beside structural factors. In addition, a metamagnetic transition can also contribute to high magnetostriction. However, in our samples, as can be observed in the field dependence of magnetization measurements, the magnetization up to 7.5 MA/m (9 T) is very small (~1 Am^2 /kg ~1 emu/g at 9 T) and no metamagnetic transition up to 9 T was observed. The low magnetization in our samples can be one of the reasons for the low value of magnetostriction obtained in this paper.

On the other hand, different magnetostriction values of as-cast $Mn_{50}Fe_{50}$ alloy are reported in [4] and [5], which values are 500 and 300 ppm, respectively. It seems that the preparation process of the samples has influenced the magnetostriction values.

Fig. 8 shows the longitudinal and transverse magnetostrictions (at room temperature) measured on all samples subjected to cold rolling degree of 70% with true strain of ~1.2. With cold-rolling deformation, the average magnetostriction continued being around zero for all concentrations 38%–55% Mn. Ma et al. [4] had found a giant magnetostriction of 2100 ppm when their sample with nominal 50% Mn concentration was subjected to cold rolling, and to some extent even before cold rolling. They explained that this improved magnetostriction is due to the formation of a {011} <01–1> texture component. As in [4], our samples remained single γ -phase.

The texture analysis of samples with Mn contents up to 42% showed no distinct texture, whereas in those from 46% to 50% Mn a texture component {110}<1–12> has been clearly observed.

With 55% Mn, however, another texture component {011}<01–1> (with about the same intensity) has been observed, which corresponds to that found in [4].

Conclusion

The magnetic behavior of polycrystalline $Fe_{100-x}Mn_x$ alloys with x = 38, 42, 46, 50, and 55, was investigated. All samples were antiferromagnetic between 100 and 400 K. For x = 38, susceptibility measurements indicate the existence of free Mn, however, this is not visible in the XRD pattern. According to the XRD experiment, the samples exhibit a single γ -phase. Magnetostriction measurements on all samples in the as-cast state

as well as after the cold rolling process gave a (nearly) zero magnetostriction value. For 46%–50% Mn, a texture component {110} <1–12> was found, but even the texture component {011} <01–1> found for 55% Mn did not cause an enhancement of the magnetostriction up to an applied field of 2 MA/m on our sample. This is in strong contradiction to the published data on $Fe_{50}Mn_{50}$ alloy [4]. The origin of the large discrepancy between our results and the published data concerning high magnetostriction values in these alloys is very unclear.

References

[1] Y. Endoh and Y. Ishikawa, “Antiferromagnetism of γ iron manganese alloys,” J. Phys. Soc. Jpn., vol. 30, no. 4, pp. 1614–1627, Apr. 1971.

[2] W. Y. Peng and J. H. Zhang, “Magnetostriction studies in an antiferromagnetic polycrystalline Mn42Fe58 alloy,” Appl. Phys. Lett., vol. 89, no. 26, pp. 262501-1–262501-3, Dec. 2006.

[3] J. Zhang, T. Ma, A. He, and M. Yan, “Structure, magnetostrictive, and magnetic properties of head-treated Mn42Fe58 alloys,” J. Alloys Compounds, vol. 485, pp. 510–513, Jan. 2009.

[4] T. Ma, J. Zhang, H. He, and M. Yan, “Improved magnetostriction in cold-rolled and annealed Mn50Fe50 alloy,” Scripta Mater., vol. 61, no. 4, pp. 427–430, Apr. 2009.

[5] A. He, T. Ma, J. Zhang, W. Luo, and M. Yam, “Antiferromagnetic

Mn50Fe50 wire with large magnetostriction," J. Magn. Magn. Mater., vol. 321, no. 22, pp. 3778–3781, 2009.

[6] M. Rotter, H. Müller, E. Gratz, M. Doerr, and M. Loewenhaupt, "A miniature capacitance dilatometer for thermal expansion and magnetostriction," Rev. Sci. Instrum., vol. 69, no. 7, pp. 2742–2746, Jul. 1998.

[7] P. Villars and L. D. Calvert, Pearson's Handbook of Crystallographic Data for Intermetallic Phases, 2nd ed. Metals Park, OH, USA: ASM, 1991.

[8] F. Cardarelli, Materials Handbook: A Concise Desktop Reference, 2nd ed. New York, NY, USA: Springer-Verlag, 2008.